Early anthropogenic CH_4 emissions and the variation of CH_4 and $^{13}CH_4$ over the last millennium

S. Houweling,[1,2] G. R. van der Werf,[3] K. Klein Goldewijk,[4] T. Röckmann,[2] and I. Aben[1]

[1]   This study presents a new hypothesis to explain the observed variation of CH_4 and δ^{13}C-CH_4 over the last millennium. It was originally proposed that the observed minimum of δ^{13}C-CH_4 prior to the start of industrialization is caused by a large shift in biomass burning emissions between 1400 and 1700 A.D. According to our new hypothesis, however, the δ^{13}C-CH_4 minimum is the first sign of the global rise of anthropogenic CH_4 emissions. The main idea is that emissions of isotopically depleted CH_4, from, for example, rice cultivation, domestic ruminants, and waste treatment started increasing earlier than the isotopically enriched emissions from fossil fuel, which started with the start of industrialization. However, because the observed increase of atmospheric methane only started around 1750 A.D., these preindustrial anthropogenic emissions must have been accompanied by a net reduction of natural CH_4 sources during the Little Ice Age (LIA) compensating for the increase of anthropogenic emissions during that period. Results of transient box model simulations for the last millennium show that under the new hypothesis a close agreement can be obtained between model and measurements. Prior to 1400 A.D., low emissions from anthropogenic biomass burning require a sizable contribution of methane emissions from vegetation to explain the observed high level of δ^{13}C-CH_4. During the Little Ice Age, a larger than expected reduction of natural sources is needed, which calls for further verification using a more sophisticated modeling approach and additional constraints from ice core measurements.

Citation: Houweling, S., G. R. van der Werf, K. Klein Goldewijk, T. Röckmann, and I. Aben (2008), Early anthropogenic CH_4 emissions and the variation of CH_4 and $^{13}CH_4$ over the last millennium, *Global Biogeochem. Cycles*, *22*, GB1002, doi:10.1029/2007GB002961.

1.   Introduction

[2]   At present, methane (CH_4) is the second most important increasing greenhouse gas with an estimated radiative forcing of 0.48 ± 0.05 Wm^{-2} [*Intergovernmental Panel on Climate Change*, 2007]. This radiative forcing is well constrained because the preindustrial and the present day global mean methane mixing ratios are accurately quantified. However, to predict future climate change requires detailed understanding of the various processes controlling methane, including natural processes and their feedbacks to climate change. This is a field of active scientific research where the uncertainties are large.

[3]   In recent years the methane mixing ratio in the atmosphere has stabilized [*Dlugokencky et al.*, 2003] and

several processes have been suggested as an explanation. Emissions from natural gas production have likely declined owing to the collapse of the economy in the former Soviet Union in the early 1990s. Developed countries show stabilizing or decreasing emissions from several sources, including coal production, landfills, and cattle. These processes could have compensated continued emission increases in developing countries [*Olivier*, 2002; *van Aardenne et al.*, 2005]. However, inverse modeling results by *Bousquet et al.* [2006] suggest that the recent stabilization is only a temporary phenomenon, caused by temporarily decreased wetland emissions compensating for structurally increasing fossil emissions. On the contrary, *Keppler et al.* [2006] speculate that the recent decrease in growth rate might be explained by large-scale tropical deforestation reducing methane emissions from vegetation, which will likely continue in the future. These studies nicely illustrate the current confusion about the future of methane, caused, in part, by insufficient understanding of its natural sources.

[4]   To improve estimates of natural methane emissions on the global scale, historic variations of the methane mixing ratio are studied. Measurements on ice and firn [*Etheridge et al.*, 1998; *MacFarling Meure et al.*, 2006] convincingly demonstrate that the preindustrial, and supposedly undisturbed, methane level was about a factor 2.5 lower than

[1]Netherlands Institute for Space Research (SRON), Utrecht, Netherlands.

[2]Institute for Marine and Atmospheric Research Utrecht, Utrecht University, Utrecht, Netherlands.

[3]Faculty of Earth and Life Sciences, Vrije Universiteit Amsterdam, Amsterdam, Netherlands.

[4]Netherlands Environmental Assessment Agency (MNP), Bilthoven, Netherlands.

today. The preindustrial CH_4 mixing ratio of ~700 ppb has been used in the past to estimate the source strength of natural wetlands [*Chappellaz et al.*, 1993; *Houweling et al.*, 2000], which was considered the dominant process in absence of anthropogenic sources. Those top-down estimates, however, have become increasingly uncertain after the discovery of methane emissions from plants [*Keppler et al.*, 2006].

[5] Ice core measurements of the historic variation of stable isotope ratios in methane provide additional process specific information, because the different sources emit at process-specific isotopic ratios. The first measurements of $\delta^{13}C$-CH_4 for the period $0-2000$ A.D. [*Ferretti et al.*, 2005] show two unexpected features: (1) a medieval $\delta^{13}C$ level of $\sim-47‰$ close to the present value and (2) a pronounced minimum at $\sim-49‰$ around 1800 A.D. In contrast, a wetland dominated CH_4 budget implies a fairly constant preindustrial level of $\delta^{13}C$ at $\sim-50‰$ [*Houweling et al.*, 2000]. Two hypotheses have been put forward to explain the measurements: [*Ferretti et al.*, 2005] propose that the high medieval $\delta^{13}C$-CH_4 level is caused by a high level of preindustrial biomass burning, which they attribute to the intensive use of fire by native population of North and South America. The decrease in $\delta^{13}C$-CH_4 between 1400 and 1700 A.D. is explained in part by the European colonists who decimated the native population, thereby significantly reducing the use of fire. Alternatively, *Keppler et al.* [2006] attribute the high medieval $\delta^{13}C$-CH_4 level to CH_4 emissions from vegetation, however, they do not provide an explanation for the observed minimum.

[6] Additional isotopic evidence is provided by [*Schaefer et al.*, 2006] who measured $\delta^{13}C$-CH_4 during the last glacial-interglacial transition. According to their measurements, $\delta^{13}C$-CH_4 remained at a fairly constant level of $\sim-46‰$ between the Younger Dryas and the Preboreal, during which CH_4 itself increased by 250 ppb. Since we can safely rule out any significant anthropogenic influence in this period, it can be concluded that the high preindustrial $\delta^{13}C$-CH_4 level reflects natural conditions. Furthermore, these measurements and similar data from *Sowers* [2006] for CH_3D suggest that the isotopic composition of natural CH_4 is rather insensitive to large climatic variations.

[7] In this study, an alternative scenario is proposed to explain the observed variation of CH_4 and $\delta^{13}C$-CH_4 over the last millennium. It starts from the notion that, in a period of rapid societal and technological developments and a significant increase of the global population, anthropogenic perturbations are more likely to originate from an increase of human-related emissions rather than a decrease as suggested by *Ferretti et al.* [2005]. In fact, the observed $\delta^{13}C$-CH_4 curve resembles an exponential function, except that it switches sign in the 19th century. Looking closer, it could be a superposition of two exponentially increasing functions, one negative, one positive, with the second starting later and quickly dominating the first. The hypothesis is that these functions reflect different stages of human development, the first dominated by agriculture (characterized by isotopically light CH_4 sources, such as cattle, rice cultivation and organic waste) and the second by industry (characterized by isotopically heavy fossil sources). This scenario has two further implications: (1) The high prebor-

eal and medieval $\delta^{13}C$-CH_4 level cannot be explained by natural biomass burning only and must have another cause, which in our simulations is CH_4 emission from vegetation, and (2) a reduction of natural sources during the Little Ice Age initially masked the increase of anthropogenic sources. The second implication follows from the fact that the CH_4 mixing ratio increase started only around 1750 A.D. We performed transient box model calculations for the period $1000-2000$ A.D. showing that this hypothesis can explain the CH_4 and $\delta^{13}C$-CH_4 measurements.

[8] The structure of this paper is as follows: First, we will describe the applied emission scenarios, followed by a brief outline of the box model. In section 4 the results of the box model calculations are compared with the measurements, including sensitivity experiments. Section 5 summarizes the main outcome and the overall conclusions.

2. Historic Methane Emissions

2.1. Anthropogenic Emissions

[9] Anthropogenic methane emissions for the period $1890-1990$ are taken from EDGAR-HYDE 1.4 [*van Aardenne et al.*, 2001]. The emissions per process are scaled such that the 1990 values correspond to scenario S3 of *Houweling et al.* [2006]. Additional assumptions are needed to account for anthropogenic emissions prior to 1890 A.D., which are not covered by the existing historic emission reconstructions. For nonfossil anthropogenic emissions it seems reasonable to assume a tight relationship with economic and demographic development. Here this is represented by an exponential fit to population statistics [*Klein Goldewijk*, 2001], translated to methane emissions by assuming a negligible anthropogenic source by 0 A.D. and the scaled EDGAR-HYDE 1.4 estimate of 90 Tg CH_4 a^{-1} by 1890 A.D. (see Figure 1). Fossil-fuel emissions prior to 1890 A.D. have been scaled to fossil CO_2 emissions, taken from a compilation by G. Marland et al. (see http://cdiac. ornl.gov/trends/emis/em_cont.htm) covering the period $1751-2003$. This approach yields very low emissions for 1750 A.D. (<1 Tg CH_4 a^{-1}), so we can safely neglect any contribution of fossil fuel before that time.

[10] Contemporary CH_4 biomass burning emissions are calculated using satellite-derived burned area and fuel loads as in work by *van der Werf et al.* [2006]. For this study, we averaged FPAR and burned fraction over the $1997-2004$ period per continent, latitude, and HYDE land cover class [*Klein Goldewijk*, 2001]. The results are projected back in time using the historical HYDE land cover and population density maps [*Klein Goldewijk*, 2001]. With averaged input data, we calculated contemporary CH_4 emissions to be 34 Tg CH_4 a^{-1}, significantly higher than the 21 Tg CH_4 a^{-1} as calculated by *van der Werf et al.* [2006]. The difference is mainly caused by the averaging of burned fractions over larger regions. With increasing fire frequency, fuel loads become smaller as the time for biomass accumulation is shorter. Fire frequencies show considerable spatial heterogeneity so averaging burned fractions will increase emissions. The higher biomass burning emissions, however, are not necessarily less realistic as several studies employing inversion techniques using satellite-derived CO have
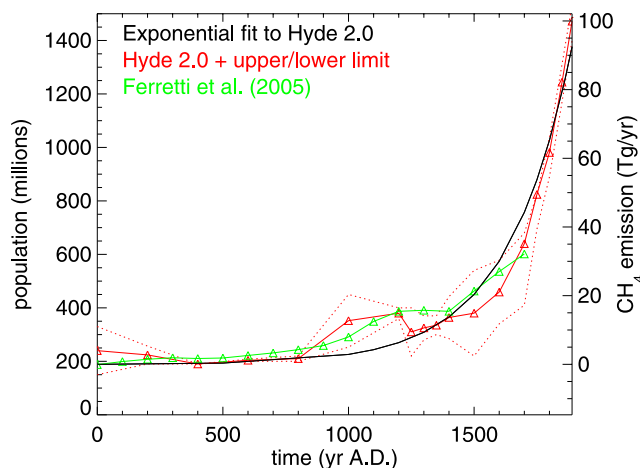
Figure 1. Estimated global demographic development in the period 0–1890 A.D. and corresponding nonfossil anthropogenic CH$_4$ emissions.

shown that the emissions by *van der Werf et al.* [2006] were probably an underestimate [see, e.g., *Arellano et al.*, 2006; *Gloudemans et al.*, 2006]. To preserve overall consistency with the S3 scenario of *Houweling et al.* [2006] we choose to rescale the calculated emissions to 30 Tg CH$_4$ a^{-1}, which yields 40 Tg CH$_4$ a^{-1} for global biomass burning after including 10 Tg CH$_4$ a^{-1} from biofuel burning.

[11] It is challenging to estimate historic fire emissions owing to a lack of data on historical fire frequencies. Information is available for temperate regions based on tree ring data [e.g., *Swetnam*, 1993], and *Mouillot et al.* [2006] estimated global fire emissions for the 1900–2000 period. In general, fire frequencies have decreased over time in temperate ecosystems owing to diminishing use of fire as a land management tool and because of increased fire fighting, while fire frequencies have increased in tropical ecosystems owing to higher population that increasingly uses fire as a tool for land management and deforestation. To capture these dynamics, we scaled our burned fractions back in time not only on the basis of historical land use but also on the basis of historical population density. For tropical forest regions, burned fractions were scaled linearly back in time with population density, as fires rarely happen in tropical forest in natural state. In tropical savanna and forest regions population density determined only half the fire frequency, as these regions have a high fire frequency also in natural state [e.g., *Van Wilgen et al.*, 2004]. *Van Wilgen et al.* [2004] showed that fires are usually set by humans before they are ignited by lightning, thus suggesting that the natural fire frequency is lower than at present. They also noted that several other factors influence fire frequency, including precipitation rates which govern the amount of fuel, and herbivory. However, for lack of any quantitative information these drivers were assumed constant.

[12] Our approach yields a similar trend for the 1900–2000 period as found by *Mouillot et al.* [2006], although our emission increase is somewhat larger because of a lower contribution of savanna emissions due to lower fuel loads. The lower fuel loads were the result of including herbivory

and fuel wood collection in our modeling approach. In the boreal region we assumed no changes except for those caused by change in historic land use, which were small. *Mouillot et al.* [2006] found higher emissions in boreal America and Asia in 1900 than in the late 20th century, but we argue that our data includes recent high boreal fire years (1998, 2002, 2003) and our climatology may therefore be higher than average. However, there may have been a decrease in fire emissions from this region in the middle of the 20th century that is not captured in our modeling approach. In temperate regions, we assumed that fire frequencies were inversely related to population density, leading to decreasing emissions at these latitudes. This only slightly retards the global increase because emissions from temperate regions are an order of magnitude smaller than tropical emissions. Also note that high preindustrial fire frequencies in temperate regions, especially in the United States, may not have been as widespread as often assumed [*Swetnam and Baisan*, 1993]. Figure 2 shows our reconstructed historic time series of anthropogenic methane emissions (including biomass burning), which increase from 20 to 370 Tg CH$_4$ a^{-1} over the period 1000 to 2000 A.D.

2.2. Natural Emissions

[13] Natural methane emission are taken from scenario S3 of *Houweling et al.* [2006], but are modified to account for climatic variations over the last millennium as described in this section. In section 1 we argued that natural sources of methane should have decreased during LIA to counteract rising anthropogenic emissions. For biomass burning this assumption is supported by ubiquitous evidence of increased biomass burning during anomalously warm and dry years [*van der Werf et al.*, 2004], so a less frequent occurrence of such conditions during LIA likely led to lower emissions. In the case of wetlands, CH$_4$ emissions depend on several factors including temperature and precipitation. The assumption, which we will verify later in this section, is that during LIA temperature effects were dominant. For vegetation emissions no temperature dependence
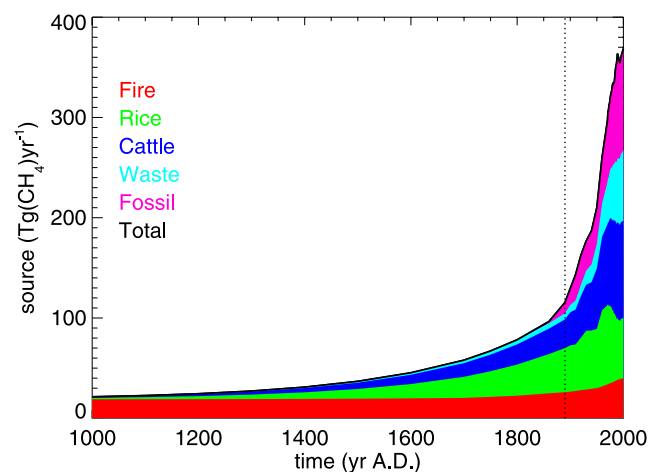

Figure 2. Estimated anthropogenic emissions of CH$_4$ over the last millennium. Biomass burning emissions represent the global total, including the natural component.

Table 1. Overview of Climate Sensitivity Parameter Settings

Simulation	Q_{10}	α
CS1	1	1
CS2	6	1
CS3	10	1.5
CS4	20	1.5

has yet been measured, except for emissions from plant litter, which, however, contribute only a small amount [*Keppler et al.*, 2006]. In conclusion, the evidence for reduced natural emissions during LIA is not strong, but it is not an unrealistic possibility either. In our calculations, lacking sophisticated relationships between natural emissions and climate, we use the highly simplified equation

$$E_i'(t) = E_i(t)Q_{10}^{\alpha(T_{NH}(t)-T_{NH}(1990))/10}. \tag{1}$$

$E_i'(t)$ and $E_i(t)$ are time-dependent emissions, respectively, with and without climate correction, for process i, where i denotes either biomass burning, natural wetlands or vegetation. The temperature sensitivity is expressed by a Q_{10} relation. In absence of further evidence we use the same Q_{10} value for each process. $T_{NH}(t)$ is the time-dependent annual mean Northern Hemispheric (NH) temperature taken from the historic temperature reconstruction of *Moberg et al.* [2005]. The historic temperature variability is scaled by a factor α to account for uncertainties in the temperature reconstruction and differences between the NH mean and the average temperature to which methane sources are exposed. The climate sensitivity of the methane emissions is varied over a wide range in separate model simulations (CS1–CS4), using the Q_{10} and α values listed in Table 1.

[14] For vegetation, in addition to temperature, land use change can be expected to have influenced the global emissions. This has been accounted for by coupling the land cover classes used by *Klein Goldewijk* [2001] to the vegetation class-specific methane emissions provided by *Keppler et al.* [2006]. Subsequently, the historic land use change maps by *Klein Goldewijk* [2001] have been used to derive historic changes in vegetation emission. In absence of land use estimates prior to 1700 A.D. a potential vegetation map is used neglecting any potential land-use change that might have occurred until then (amounting to ~5% of the global land area in 1700 A.D.). Land use change has certainly also affected natural wetland emissions, but this is poorly documented for the global scale. A global review in framework of the Ramsar convention on wetland conservation points to a 50% reduction in wetland area since 1900 [*Finlayson and Spiers*, 1999]. However, such a large decrease seems difficult to reconcile with the observed increase in methane during this period. Since it is unclear how the combined effects of climate and land use change have influenced wetland emissions during the 20th century we apply equation (1) without further assumptions. For biomass burning emissions, the temperature correction is applied to the historic emissions explained in section 2.1.

[15] Figure 3 summarizes the resulting historic emissions per process and climate scenario. Overall, the applied climate sensitivity settings result in natural sources that are reduced by 0% (CS1) to 25% (CS4) during LIA

compared with 1000 A.D. Emissions from vegetation and wetlands are of roughly similar magnitude and vary between 60 and 80 Tg CH_4 a^{-1}. Biomass burning emission increase from 20 Tg CH_4 a^{-1} preindustrially to 40 Tg CH_4 a^{-1} at present. Biomass burning is included in both Figures 2 and 3, although we do not distinguish between natural and anthropogenic contributions. The only difference between the biomass burning estimates in Figures 2 and 3 is the impact of climatic variations (the values in Figure 2 correspond to those for CS1 in Figure 3).

[16] To verify the assumed response of wetland emissions to climate variability multiannual simulations have been performed with the wetland model by *Walter and Heimann* [2000], covering the last millennium in 10-year intervals. The historic variations in precipitation, temperature and net primary production needed for these simulations are taken from output of the Bern Carbon cycle–Climate (Bern CC) model [*Gerber et al.*, 2003]. In these simulations, the annual mean Northern Hemispheric temperature is rescaled to match the temperature reconstruction by [*Moberg et al.*, 2005]. Figure 4 shows wetland emissions calculated using this approach, smoothed using a Gaussian filter with a σ of 30 years to remove short-term variability. The results confirm that wetland emissions prior to 1900 A.D. are influenced mostly by changes in temperature. The limited influence of precipitation is explained by the fact that the climate model does not show a significant large-scale variation in precipitation on the timescale of several decades or longer. The simulations show a 5 Tg CH_4 a^{-1} reduction during the Little Ice Age in response to temperature decrease. Interestingly, the prescribed NPP variations, excluding land use change, cause a 10 Tg CH_4 a^{-1} increase of wetland emissions after 1900 A.D. As explained earlier, however, wetland drainage probably caused reductions by similar amounts or more. The results of the wetland model
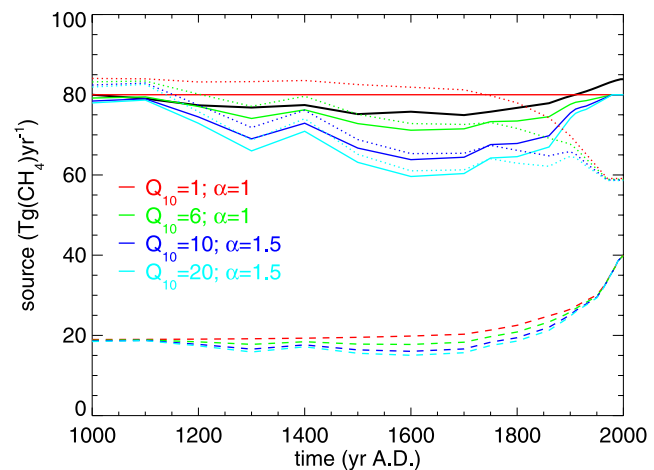

Figure 3. natural Emissions Of CH_4 Over The Last Millennium For A Range Of Temperature Sensitivities (Red–Blue). Lines Denote: Solid Line, Wetlands; Dashed Line, Biomass Burning; And Dotted Line, Vegetation. The Solid Black Line Shows CH_4 Emissions Calculated Using The *Walter And Heimann* [2000] Wetland Model. Biomass Burning Emissions Represent The Global Total, Including The Anthropogenic Component.
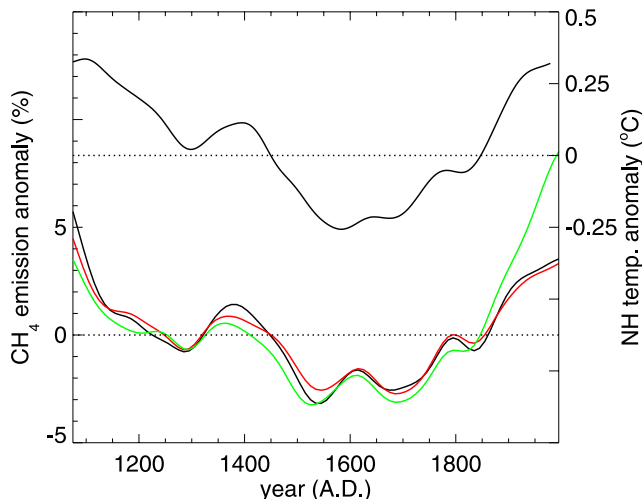
Figure 4. Comparison of the estimated variability of NH temperature according to *Moberg et al.* [2005] (top line) and the variability of CH_4 emissions from wetlands using the *Walter and Heimann* [2000] model (bottom lines). Model calculations are driven by: black, GCM calculated temperature variations with NH-mean temperature scaled to *Moberg et al.* [2005]; red, as black plus GCM calculated precipitation variations; and green, as red plus Bern CC-derived NPP variations.

simulation accounting for precipitation and NPP variations have been plotted in Figure 3 for comparison with the results obtained using equation (1). It shows that the climate sensitivity of the *Walter and Heimann* [2000] model most closely resembles that of CS2, which is consistent with the fact that both the process model and SC2 assume a Q_{10} of 6.

3. Model Description

[17] The temporal evolutions of atmospheric CH_4 and $\delta^{13}C$-CH_4 are calculated using a single box representing the

global atmosphere. This is adequate since CH_4 has a long lifetime ($\sim$9 years) and we are only interested in global mean mixing ratios. The active variables are the global mean mixing ratio of CH_4 and $^{13}CH_4$, for which we solve the equation

$$\frac{\delta C_x(t)}{\delta t} = \frac{1}{m_{air}} \sum_i E_{x,i}(t) - \sum_j S_{x,j}(t) C_x(t), \qquad (2)$$

where $C_x(t)$ is the mixing ratio of $x (= CH_4$ or $^{13}CH_4$). $E_x(t)$ and $S_x(t)$ represent the annual source and sink strengths of x per process i and j, and m_{air} is the globally integrated mass of the atmosphere. The sources have been outlined in section 2 and the sinks have been taken from *Houweling et al.* [2000]. The prescribed OH sink accounts for a 7.5% decrease of OH since preindustrial times. The following isotopic fractionations have been applied for the sinks: 3.9‰ for OH [*Saueressig et al.*, 2001], 12‰ for the stratosphere [*Brenninkmeijer et al.*, 1995] and 22‰ for soil oxidation [*Tyler et al.*, 1994].

4. Model Results and Discussion

[18] Box model simulations have been carried out for the period 0–2000 A.D., however, only results for the last millennium will be analyzed and discussed. The 1000-year spin-up guarantees that the results are independent of the initial conditions (at negligible CPU costs). Figure 5 shows comparisons of measured and model simulated time series of CH_4 and $\delta^{13}C$-CH_4. CH_4 measurements are taken from *Etheridge et al.* [1998] (average of data from Greenland and Antarctica) and *MacFarling Meure et al.* [2006] (Antarctica only). From model-derived 3D CH_4 fields [*Houweling et al.*, 2006] it follows that the difference between the global mean (as obtained using a box model) and Antarctica is smaller than the difference between the observed CH_4 time series presented in Figure 5. For $\delta^{13}C$-CH_4 the difference between the global mean and Antarctica is within 0.2‰.
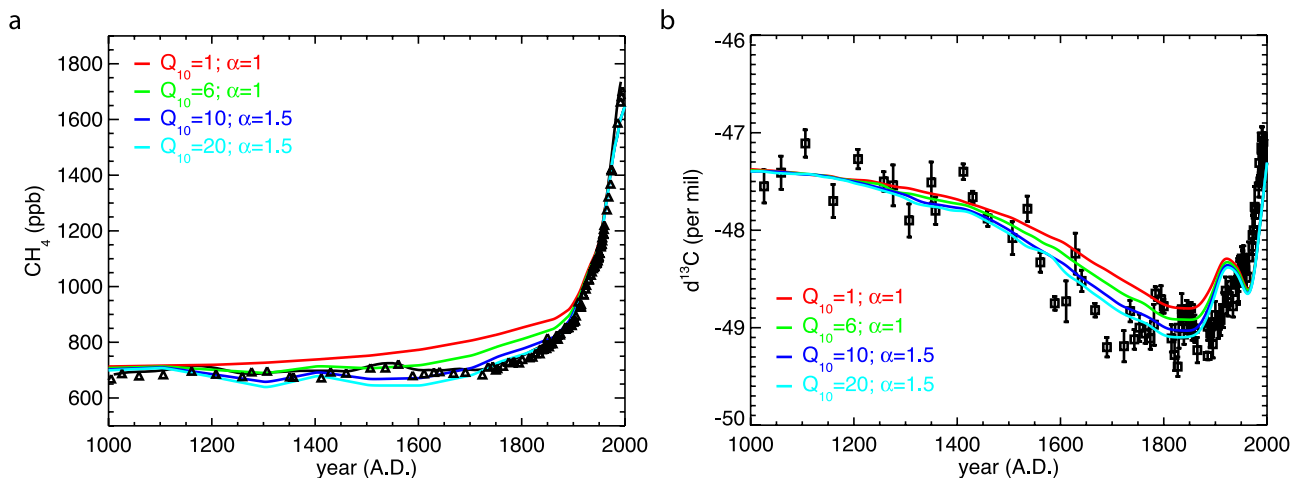

Figure 5. Comparison of simulated and measured (a) CH_4 and (b) $^{13}CH_4$ for the last millennium. CH_4 measurements are represented by triangles [*MacFarling Meure et al.*, 2006] and a black line [*Etheridge et al.*, 1998]. Squares represent measured $\delta^{13}C$-CH_4 plus 1σ uncertainty [*Ferretti et al.*, 2005]. Colored lines represent box model simulations with temperature sensitivity increasing from red to light blue (CS1–CS4).

[19] Overall the model reproduces the observed time evolutions satisfactorily. This is in particular true for δ^{13}C-CH$_4$, which has been most troublesome to explain in the past. In the 20th century the model shows a more variable trend in δ^{13}C-CH$_4$ than the measurements. Similar differences, although less pronounced, were reported by *Lassey et al.* [2006]. The interruption of the δ^{13}C-CH$_4$ increase around 1950 is caused by a reduction in the growth rate of fossil CH$_4$ between 1930 and 1950, while other anthropogenic sources, notably emissions from cattle, continued to increase.

[20] The results in Figure 5 point to CS3 as the most realistic climate sensitivity. However, according to Figure 3 this implies a climate sensitivity that is about twice as high as predicted by the *Walter and Heimann* [2000] wetland model. For wetlands, the Q_{10} of 10 used in CS3 is indeed high, although still within the range of 1.6–16 reported by *Walter and Heimann* [2000]. The choice of $\alpha = 1.5$ is also pushing the temperature variations to the uncertainty limits reported by *Moberg et al.* [2005]. In fact, it may well overestimate the true temperature variation, since the long-term preindustrial temperature variation of $\sim 0.5°$C derived by *Moberg et al.* [2005] is already substantially larger than the variation of $\sim 0.2°$C reported by *Jones and Mann* [2004]. One could argue that the NH mean temperature is not representative for global methane sources. For example, temperature variations of the Arctic wetlands have likely been larger than the NH mean. In our source scenario, however, emissions from high northern latitudes do not dominate the overall budget. Nevertheless, *Jones and Mann* [2004] confirm that regional climatological variations have been substantially larger than the hemispheric mean, which adds considerable uncertainty to the preindustrial variation of natural methane emissions.

[21] The CH$_4$ results without temperature sensitivity (shown in red) are about 100 ppb higher than the measurements. This means that the required correction amounts to about 30% of the CH$_4$ difference between the Holocene and the Last Glacial Maximum. If equation (1) is extrapolated to a temperature decrease of 5°C, roughly representing glacial conditions, this leads to a methane mixing ratio of ~ 400 ppb, which is close the observed level of 350 ppb. In contrast, the studies by *Kaplan* [2002] and *Kaplan et al.* [2006] indicate that source changes alone are insufficient to explain the mixing ratio difference between glacial and interglacial methane, calling for a significant change in its atmospheric lifetime. This argument, however, may also be true for LIA. If we had treated the climate sensitivity of the OH sink similar to what is used for the natural sources, then the required sensitivity would be less. It can be concluded that the reduction of natural sources during LIA needed to compensate the increase of fossil emissions is larger than expected, which could, however, be explained by simultaneous changes in OH.

[22] The difference in δ^{13}C-CH$_4$ between the scenarios with and without temperature sensitivity remains small. However, extrapolation to the Younger Dryas to Preboreal transition would imply a ~ 1‰ change in δ^{13}C-CH$_4$ for a 250 ppb change in CH$_4$, which is larger than the observed transition [*Schaefer et al.*, 2006], although still within the

measurement uncertainty. Of course, our assumption of the same temperature sensitivity for biomass burning, wetlands and plants is rather arbitrary. Combinations are possible that make the δ^{13}C-CH$_4$ signature of the combined natural source independent of temperature. However, this doesn't significantly influence the mean temperature sensitivity needed to bring the model in agreement with both the CH$_4$ and δ^{13}C-CH$_4$ measurements.

[23] Next, we will analyze the robustness of the simulated temporal evolution of δ^{13}C-CH$_4$, in particular, with respect to the assumed anthropogenic emissions prior to 1890 A.D. Besides the standard procedure explained in section 2.1, three additional simulations are performed assuming anthropogenic emissions proportional to (1) HYDE population, (2) the lower limit of HYDE (see Figure 1), and (3) *Ferretti et al.* [2005] extended with HYDE after 1700 A.D. The CS2 climate sensitivity is used in each of these simulations.

[24] Figure 6 presents a similar comparison as Figure 5 except that now the different colors represent the different back-extrapolations of the anthropogenic emissions. Figure 6 clearly demonstrates that the shape of the simulated curve is rather sensitive to the applied extrapolation method. Direct scaling to population shifts the point from where anthropogenic emissions become important for δ^{13}C-CH$_4$ forward in time, deteriorating the agreement with the measurements. However, the climate sensitivity needed to reproduce CH$_4$ becomes also smaller. It is not quite clear why an exponential fit to population results in the most realistic simulation of δ^{13}C-CH$_4$. To explain the differences between the scenarios, the period 1400–1700 A.D. is important. The population statistics show an abrupt acceleration in population growth after ~ 1600 A.D., which is smoothed by the exponential fit. One could speculate that the fast population increase prompted for a more efficient treatment of waste, which might have reduced per capita methane emissions for this process. Of course, in rapidly developing societies many other factors change also, adding complexity to the relationship between population numbers and methane emissions. Given the limited amount of information that is available to derive more realistic estimates, this complexity translates into a considerable uncertainty.

[25] Overall, the combined uncertainty of preindustrial human emissions and the climate sensitivity of natural sources are certainly larger than the differences between our simulations and the measurements. Although in our simulations SC3 performs better than the more realistic scenario SC2, it should in principle be possible, within the uncertainties, to obtain a perfect agreement with the measurements for each of these climate sensitivity scenarios. This means that rising anthropogenic emissions can indeed explain most of the observed δ^{13}C-CH$_4$ variations, providing observational support to our hypothesis. Further confirmation should come from more detailed analyzes of natural sources, which will, among others, require improved understanding of vegetation emissions. A solid prove of the hypothesis, however, will probably require additional observational constraints. These could come from measurements of ^{13}CH$_4$, and preferably also CH$_3$D, from Antarctica and Greenland.

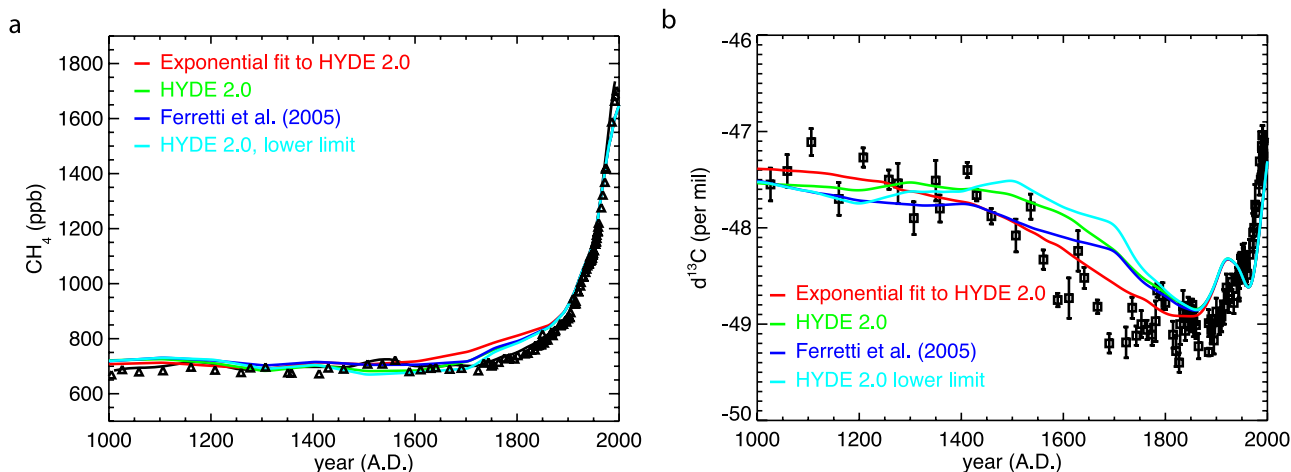**Figure 6.** Comparison of simulated and measured (a) CH_4 and (b) $^{13}CH_4$ for the last millennium. Colored lines represent model simulations using different methods to back-extrapolate the anthropogenic emissions prior to 1890 A.D. Scenario CS2 was used for the natural sources. CH_4 measurements are represented by triangles [*MacFarling Meure et al.*, 2006] and a black line [*Etheridge et al.*, 1998]. Squares represent measured δ^{13}C-CH$_4$ plus 1σ uncertainty [*Ferretti et al.*, 2005].

[26] Further, our results show that it is possible to reproduce the available CH_4 and δ^{13}C-CH$_4$ measurements assuming a large source of methane from vegetation, although it doesn't proof that the emissions should indeed be large. In fact, the results by *Keppler et al.* [2006] still await confirmation by other research groups, and are even contradicted by recent laboratory measurements reported by *Dueck et al.* [2007]. Alternatively, a high natural level of biomass burning might explain the observed medieval δ^{13}C-CH$_4$ level [*Ferretti et al.*, 2005, 2007]. However, it is difficult to imagine how preindustrial biomass burning could have been comparable to that at present, given the pressure of urbanization on ecosystems and associated increases in the average fire frequencies in tropical ecosystems. Furthermore, the emissions in deforestation regions are often the result of a highly mechanized deforestation regime, aided by heavy machinery [*Morton et al.*, 2006] that would be difficult to achieve with manpower alone. Moreover, emissions as high as contemporary emissions are not sustainable for periods longer than 100 years as they implicate an annual loss of tropical forest of about 1% per year or higher.

[27] Among the remaining uncertainties is also the isotope fractionation of the atmosphere [see, e.g., *Allan et al.*, 2001, 2005]. Unless it has changed over the last millennium it doesn't provide an explanation why medieval δ^{13}C-CH$_4$ was comparable to its present day level. However, a different fractionation does influence the mean δ^{13}C-CH$_4$ level and thereby the relative importance of emissions from vegetation, wetlands and biomass burning.

[28] The question remains what shift in emissions is needed to explain the high medieval level of $^{13}CH_4$ in absence of plant emissions and whether or not such a scenario can still explain the preindustrial δ^{13}C-CH$_4$ minimum. We attribute the preindustrial minimum to changes in anthropogenic sources, whereas the high medieval level of δ^{13}C-CH$_4$ must be caused by natural sources, which according to our hypothesis do not contribute significantly to the

preindustrial variation of δ^{13}C-CH$_4$. Owing to this separation of sources, the model can reproduce the preindustrial variation of δ^{13}C-CH$_4$ largely independently from the medieval level of δ^{13}C-CH$_4$. Without vegetation emissions, increased biomass burning emissions are needed to explain the observed level of medieval δ^{13}C-CH$_4$. To test this scenario, we attribute all vegetation emissions to biomass burning and natural wetlands under the extreme assumption that anthropogenic biomass burning replaced natural biomass burning without changing the total emissions, except for a modest increase in biofuel emissions of 5 Tg CH$_4$ a^{-1}. Then, to explain the medieval level of δ^{13}C-CH$_4$, it still requires a fractionation of the tropospheric sink of about 5.5‰ (i.e., significantly larger than the 3.9‰ used in the base scenario). If we use this scenario in our model, including our parameterization of climate variability, then a close agreement is obtained between the model and the observed CH_4 and $^{13}CH_4$ time series (not shown). Although, as explained earlier, we do not consider the assumed level of preindustrial biomass burning realistic, this experiment demonstrates that increasing preindustrial anthropogenic emissions can explain the preindustrial δ^{13}C-CH$_4$ variation, independent of specific assumptions regarding vegetation emissions.

[29] Finally, we would like to point to a remaining uncertainty that should be investigated in more detail in the future. This study and earlier studies of δ^{13}C-CH$_4$ assume that the isotopic signature of the sources have remained constant in time. It is known, however, that isotope signatures of individual sources are variable. For example, seasonal variation of the isotopic composition of methane emissions from rice cultivation have been reported by *Bergamaschi* [1997] and *Marik et al.* [2002]. Furthermore, it has been suggested that the fraction of methane from wetlands that is oxidized in the oxygen rich interface with the atmosphere is a function of climatic conditions [*Sowers*, 2006]. This could influence our δ^{13}C simulations

since the isotopic signature of methane emissions from wetlands is directly related to the fraction of oxidation. In the [*Walter and Heimann* [2000] wetland model, however, the global mean fraction of oxidation remains surprisingly constant over the last millennium.

[30] Our simulations are sensitive to a change in the isotopic composition of organic matter in response to the observed 1.5‰ decrease of the atmospheric $\delta^{13}C$ of CO_2 during industrialization [*Francey et al.*, 1999]. A changing competition between C3 and C4 grasses caused by the increase of CO_2 and global warming during the 20th century [*Collatz et al.*, 1998] may have introduced additional isotopic shifts. The extent to which this affects the isotopic composition of methane emissions depends on the mean turnover time of the carbon pools involved. Several studies indicate that the bulk of dissolved organic matter is not much older than several years [*Benner et al.*, 2004; *Trumbore and Harden*, 1997; *Mayorga et al.*, 2005]. This might have caused a systematic decrease of the isotopic composition of wetland CH_4 by ~1.5‰ since 1800 A.D. The same is probably true, to a varying extent, for most nonfossil sources of methane. How exactly a change in isotopic composition of about 1.5‰ can be accommodated in the 20th century $^{13}CH_4$ budget requires further investigation.

5. Conclusions

[31] We have presented a new explanation for the observed variation of CH_4 and $\delta^{13}C\text{-}CH_4$ over the last millennium. Our hypothesis shows that the unexpected variation in $\delta^{13}C\text{-}CH_4$ can be explained by increasing anthropogenic methane emissions over the past millennium, in combination with a shift from nonfossil to fossil sources during the industrial period. Transient box model calculations confirm that this scenario can be brought in agreement with the measurements. It requires a larger than expected decrease of natural emissions during the Little Ice Age (equivalent to ~100 ppb) to explain the observed CH_4 mixing ratios for that period, which might be explained by a change in OH. The required reduction of natural emissions is sensitive to the method that is used to extrapolate anthropogenic emissions to the period prior to 1890 A.D. Since both the pre-1890 anthropogenic emissions and the climate sensitivity of methane sources are highly uncertain we conclude that the differences between measurements and model simulations are within the uncertainties, and therefore our hypothesis may indeed be correct. Further verification calls for a more sophisticated modeling approach, including process modeling of natural methane sources. To unambiguously prove or falsify our anthropogenic emission hypothesis will probably require consistent measurements records of CH_4, $\delta^{13}C\text{-}CH_4$, and $\delta D\text{-}CH_4$ from Antarctica and Greenland.

References

Allan, W., M. R. Manning, K. R. Lassey, D. C. Lowe, and A. J. Gomez (2001), Modeling the variation of $\delta^{13}C$ in atmospheric methane: Phase ellipses and the kinetic isotope effect, *Global Biogeochem. Cycles*, *15*, 467–481.

Allan, W., D. C. Lowe, A. J. Gomez, H. Struthers, and G. W. Brailsford (2005), Interannual variation of ^{13}C in tropospheric methane: Implications for a possible atomic chlorine sink in the marine boundary layer, *J. Geophys. Res.*, *110*, D11306, doi:10.1029/2004JD005650.

Arellano, A. F., P. S. Kasibhatla, L. Giglio, G. R. van der Werf, J. T. Randerson, and G. J. Collatz (2006), Time-dependent inversion estimates of global biomass-burning CO emissions using Measurement of Pollution in the Troposphere (MOPITT) measurements, *J. Geophys. Res.*, *111*, D09303, doi:10.1029/2005JD006613.

Benner, R., B. Benitez-Nelson, K. Kaiser, and R. M. W. Amon (2004), Export of young terrigenous dissolved organic carbon from rivers to the Arctic Ocean, *Geophys. Res. Lett.*, *31*, L05305, doi:10.1029/2003GL019251.

Bergamaschi, P. (1997), Seasonal variation of stable hydrogen and carbon isotopic ratios in methane from a Chinese rice paddy, *J. Geophys. Res.*, *102*, 25,383–25,393.

Bousquet, P., et al. (2006), Contribution of anthropogenic and natural sources to atmospheric methane variability, *Nature*, *443*, 439–443, doi:10.1038/nature05132.

Brenninkmeijer, C. A. M., D. C. Lowe, M. R. Manning, R. J. Sparks, and P. F. J. van Velthoven (1995), The ^{13}C, ^{14}C, and ^{18}O isotopic composition of CO, CH_4, and CO_2 in the higher southern latitudes lower stratosphere, *J. Geophys. Res.*, *100*, 26,163–26,172.

Chappellaz, J. A., I. Y. Fung, and A. M. Thompson (1993), The atmospheric CH_4 increase since the last glacial maximum, 1, Source estimates, *Tellus, Ser. B*, *45*, 228–241.

Collatz, G. J., J. A. Berry, and J. S. Clark (1998), Effects of climate and CO_2 partial pressure on the global distribuiion of C_4 grasses: Present, passt, and future, *Oecologia*, *114*, 441–454.

Dlugokencky, E. J., S. Houweling, L. B. K. A. Masarie, P. M. Lang, J. B. Miller, and J. B. Tans (2003), Atmospheric methane levels off: Temporary pause or a new steady-state?, *Geophys. Res. Lett.*, *30*(19), 1992, doi:10.1029/2003GL018126.

Dueck, T. A., et al. (2007), No evidence for substantial aerobic methane emission by terrestrial plants: A ^{13}C-labelling approach, *New Phytol.*, *175*, 29–35, doi:10.1111/j.1469-8137.2007.02103.x.

Etheridge, D. M., L. P. Steele, R. J. Francy, and R. L. Langenfelds (1998), Atmospheric methane between 1000 A. D. and present: Evidence of anthropogenic emissions and climatic variability, *J. Geophys. Res.*, *103*, 15,979–15,993.

Ferretti, D. F., et al. (2005), Unexpected changes to the global methane budget over the past 200 0 years, *Science*, *309*, 1714–1717.

Ferretti, D. F., J. B. Miller, J. W. C. White, K. R. Lassey, D. C. Lowe, and D. M. Etheridge (2007), Stable isotopes provide revised global limits of aerobic methane emissions from plants, *Atmos. Chem. Phys.*, *7*, 237–241.

Finlayson, C. M., and A. G. Spiers (1999), Global review of wetland resources and priorities for wetland inventory, *Supervising Sci. Rep. 144*, Environ. Res. Inst. of the Supervising Sci., Canberra, ACT, Australia. (Available at http://www.wetlands.org/publication.aspx?id = 32e5c6b9-7e7f-4910-bcc3-2b9ba697af8e)

Francey, R. J., C. E. Allison, D. M. Etheridge, C. M. Trudinger, I. G. Enting, M. Leuenberger, R. L. Langenfelds, E. Michel, and L. P. Steele (1999), A 1000-year high precision record of $\delta^{13}C$ in atmospheric CO_2, *Tellus, Ser. B*, *51*, 170–193.

Gerber, S., F. Joos, P. Brügger, T. F. Stocker, M. E. Mann, S. Sitch, and M. Scholze (2003), Constraining temperature variations over the last millennium by comparing simulated and observed atmospheric CO_2, *Clim. Dyn.*, *20*, 281–299.

Gloudemans, A. M. S., M. C. Krol, J. F. Meirink, A. T. J. de Laat, G. R. van der Werf, H. Schrijver, M. M. P. van den Broek, and I. Aben (2006), Evidence for long-range transport of carbon monoxide in the Southern Hemisphere from SCIAMACHY observations, *Geophys. Res. Lett.*, *33*, L16807, doi:10.1029/2006GL026804.

Houweling, S., F. J. Dentener, and J. Lelieveld (2000), Simulation of preindustrial atmospheric methane to contrain the global source strength of natural wetlands, *J. Geophys. Res.*, *105*, 17,243–17.255.

Houweling, S., T. Röckmann, I. Aben, F. Keppler, M. Krol, J. F. Meirink, E. J. Dlugokencky, and C. Frankenberg (2006), Atmospheric constraints on global emissions of methane from plants atmospheric constraints on global emissions of methane from plants, *Geophys. Res. Lett.*, *33*, L15821, doi:10.1029/2006GL026162.

Intergovernmental Panel on Climate Change (2007), *Climate Change 2007: The Physical Science Basis—Fourth Assessment Report of the Intergo-*

vernmental Panel on Climate Change, Cambridge Univ. Press, New York.

Jones, P. D., and M. E. Mann (2004), Climate over past millennia, *Rev. Geophys.*, *42*, RG2002, doi:10.1029/2003RG000143.

Kaplan, J. O. (2002), Wetlands at the Last Glacial Maximum, *Geophys. Res. Lett.*, *29*(6), 1079, doi:10.1029/2001GL013366.

Kaplan, J. O., G. Folberth, and D. A. Hauglustaine (2006), Role of methane and biogenic volatile organic compound sources in late glacial and holocene fluctuations of atmospheric methane concentrations, *Global Biogeochem. Cycles*, *20*, GB2016, doi:10.1029/2005GB002590.

Keppler, F., J. T. G. Hamilton, M. Brass, and T. Röckmann (2006), Methane emissions from terrestrial plants under aerobic conditions, *Nature*, *439*, 187–191, doi:10.1038/nature04420.

Klein Goldewijk, K. (2001), Estimating global land use change over the past 300 years: The HYDE database, *Global Biogeochem. Cycles*, *15*, 417–433.

Lassey, K. R., D. M. Etheridge, D. C. Lowe, A. M. Smith, and D. F. Ferretti (2006), Centennial evolution of the atmospheric methane budget: What do the carbon isotopes tell us?, *Atmos. Chem. Phys. Discuss.*, *6*, 4995–5038.

MacFarling Meure, C., D. Etheridge, C. Trudinger, P. Steele, R. Langenfelds, T. van Ommen, A. Smith, and J. Elkins (2006), Law dome CO_2, CH_4 and N_2O ice core records extended to 2000 years BP, *Geophys. Res. Lett.*, *33*, L14810, doi:10.1029/2006GL026152.

Marik, T., H. Fischer, F. Conen, and K. Smith (2002), Seasonal variations in stable carbon and hydrogen isotope ratios in methane from rice fields, *Global Biogeochem. Cycles*, *16*(4), 1094 doi:10.1029/2001GB001428.

Mayorga, E., A. K. Aufdenkampe, C. A. Masiello, A. V. Krusche, J. I. Hedges, P. D. Quay, J. E. Richey, and T. A. Brown (2005), Young organic matter as a source of carbon dioxide outgassing from Amazonian rivers, *Nature*, *436*, 538–541, doi:10.1038/nature03880.

Moberg, A., D. M. Sonechkin, K. Holmgren, N. M. Datsenko, and W. Karen (2005), Highly variable Northern Hemisphere temperatures reconstructed from low- and high-resolution proxy data, *Nature*, *433*, 613–617.

Morton, D. C., R. S. DeFries, Y. E. Shimabukuro, L. O. Anderson, E. Arai, F. del Bon Espirito-Santo, R. Freitas, and J. Morisette (2006), Cropland expansion changes deforestation dynamics in the southern Brazilian Amazon, *Proc. Natl. Acad. Sci., U. S. A.*, *103*, 14,637–14,641, doi:10.1073/pnas.0606377103.

Mouillot, F., A. Narasimha, Y. Balkanski, J.-F. Lamarqe, and C. B. Field (2006), Global carbon emissions from biomass burning in the 20th century, *Geophys. Res. Lett.*, *33*, L01801, doi:10.1029/2005GL024707.

Olivier, J. G. J. (2002), On the quality of global emission inventories, Ph.D. thesis, Utrecht Univ., Utrecht, Netherlands.

Saueressig, G., J. N. Crowley, P. Bergamaschi, C. Brühl, C. A. M. Brenninkmeijer, and H. Fischer (2001), Carbon 13 and D kinetic isotope effects in the reaction of CH_4 with O (^{1}D) and OH: New laboratory measurements and their implications for the isotopic composition of stratospheric methane, *J. Geophys. Res.*, *106*, 23,127–23,138.

Schaefer, H., M. J. Whiticar, E. J. Brook, V. V. Petrenko, D. F. Ferretti, and J. P. Severinghaus (2006), Ice record of δ^{13}C for atmospheric CH_4 across the Younger Dryas–Preboreal transition, *Science*, *313*, 1109–1112.

Sowers, T. (2006), Late Quaternary atmospheric CH_4 isotope record suggests marine clathrates are stable, *Science*, *311*, 838–840.

Swetnam, T. W. (1993), Fire history and climate-change in Giant Sequoia groves, *Science*, *262*, 885–889.

Swetnam, T. W., and C. H. Baisan (1993), Tree-ring reconstructions of fire and climate history in the Sierra Nevada and southwestern United States, in *Fire and Climatic Change in Temperate Ecosystems of the Western Americas*, *Ecol. Stud.*, vol. 160, edited by T. T. Veblen et al., pp. 158–195, Springer, New York.

Trumbore, S. E., and J. W. Harden (1997), Accumulation and turnover of carbon in organic and mineral soils of the BOREAS northern study area, *J. Geophys. Res.*, *102*, 28,817–28,830.

Tyler, S. C., P. M. Crill, and G. W. Brailsford (1994), ^{13}C/^{12}C fractionation of methane during oxidation in a temperate forested soil, *Geochim. Cosmochim. Acta*, *58*, 1625–1633.

van Aardenne, J. A., F. J. Dentener, J. G. J. Olivier, C. G. M. Klein Goldewijk, and J. Lelieveld (2001), A 1° × 1° resolution data set of historical anthropogenic trace gas emissions for the period 1890–1990, *Global Biogeochem. Cycles*, *15*, 909–928.

van Aardenne, J. A., F. J. Dentener, J. G. J. Olivier, J. A. H. W. Peters, and L. N. Ganzeveld (2005), The EDGAR 3.2 fast track 2000 dataset (32FT2000), technical report, Joint Res. Cent. (JRC), Ispra, Italy. (Available at http://www.mnp.nl/edgar/model/v32ft2000edgar)

van der Werf, G. R., J. T. Randerson, G. J. Collatz, L. Giglio, P. S. Kasibhatla, A. F. Arellano Jr., S. C. Olsen, and E. S. Kasischke (2004), Continental-scale partitioning of fire emissions during the 1997 to 2001 El Niño/-La Nina period, *Science*, *303*, 73–76.

van der Werf, G. R., J. T. Randerson, L. Giglio, G. J. Collatz, P. S. Kasibhatla, and A. F. Arellano (2006), Interannual variability in global biomass burning emissions from 1997 to 2004, *Atmos. Chem. Phys.*, *6*, 3423–3441.

Van Wilgen, B. W., et al. (2004), Response of savanna fire regimes to changing fire-management policies in a large African national park, *Conserv. Biol.*, *18*, 1533–1540.

Walter, B. P., and M. Heimann (2000), A process-based, climate-sensitive model to derive methane emissions from natural wetlands: Application to five wetland sites, sensitivity to model parameters, and climate, *Global Biogeochem. Cycles*, *14*, 745–765.

————————————————

I. Aben, Netherlands Institute for Space Research (SRON), Sorbonnelaan 2, NL-3584 CA Utrecht, Netherlands. (i.aben@sron.nl)

S. Houweling and T. Röckmann, Institute for Marine and Atmospheric Research Utrecht, Princetonplein 5, NL-3584 CC Utrecht, Netherlands. (s.houweling@phys.uu.nl; t.roeckmann@phys.uu.nl)

K. Klein Goldewijk, Netherlands Environmental Assessment Agency (MNP), P.O. Box 303, NL-3720 AH Bilthoven, Netherlands. (kees.klein.goldewijk@mnp.nl)

G. R. van der Werf, Faculty of Earth and Life Sciences, Vrije Universiteit Amsterdam, De Boelelaan 1085 NL-1081 HV Amsterdam, Netherlands. (guido.van.der.werf@falw.vu.nl)